

Fig. 1 Comparison of boundary layer and inviscid flow model profiles with vectored and normal injection

The second point of disagreement involves the source of the vorticity in the inner layer. Vinokur apparently associates this with "losses" in the injection process. Whether this relates to degradation of total pressure through the porous material or not is unclear to the authors. The authors' statement in a footnote on p. 825 of Ref. 2 attributes the rotationality in the inner layer to shear stresses. This point of view is substantiated by the boundary layer analysis of Fox and Libby.³ There the relation between the boundary layer solutions and those given by the inviscid model of Vinokur and of the authors was demonstrated for "thin" inner layers. Conceptually, there is no reason why the relation between analyses including viscosity and those based on the model in question should be altered when the inner layer is thick compared to the usual shock stand-off distance.

It is, of course, true that "vectoring" will change the rotationality in the inner layer. This can be shown by an extension of the analysis of Ref. 3 to include tangential velocities at the wall; indeed the solutions of Ref. 3 can be reinterpreted to apply to vectored injection.

As an example the "free mixing" solution (solution VI of Ref. 3) can be applied to a wall flow with vectored injection so as to yield essentially irrotational flow in the inner layer. The solution identified as solution VI in Ref. 3 and tabulated in Ref. 4, which presents in extenso the numerical results given in Ref. 3, has here been extended analytically to a value of $f = f_w = -12.5$. Thus the integration yielding $\eta = \eta(\xi)$ can be carried out [cf. Eq. (29) of Ref. 3]. With the solution extended to the value of f_w just given, the velocity distributions with vectored injection can be compared to solution V of Ref. 3, which corresponds to the same normal velocity but with no slip at the wall.

Such a comparison is shown in Fig. 1 along with the corresponding velocity distributions given by the inviscid model. It will be noted, as may be expected on physical grounds, that "vectoring" reduces the thickness of the inner layer. Of significance for the present discussion is the sensibly irrotational nature of the inner layer with "vectoring." Note that the shear measured by the shear function $G \sim f''$ is on the order of 10^{-5} at $\eta = 0$. Thus the rotationality in the inner layer depends on the tangential velocity at the wall;

the relevance of the "losses" related to the injection process is not clear to the authors.

The comparison shown in Fig. 1 clearly implies that the dependence of rotationality and tangential velocity at the wall is through the viscous equations of motion that are given for thin inner layers by the boundary layer equations. Thus it appears to the authors that shear in the inner layer is the source of the rotationality.

References

- ¹ Vinokur, M. and Sanders, R. W., "Inviscid hypersonic flow around spheres with mass injection," Lockheed Missiles & Space Co. LMSD/288209 (January 1960); also LMSD/288139 (January 1960).
- ² Cresci, R. J. and Libby, P. A., "The downstream influence of mass transfer at the nose of a slender cone," *J. Aerospace Sci.* 29, 815-826 (1962).
- ³ Fox, H. and Libby, P. A., "Helium injection into the boundary layer at an axisymmetric stagnation point," *J. Aerospace Sci.* 29, 921-934 (1962).
- ⁴ Fox, H. and Libby, P. A., "Helium injection into the boundary layer at an axisymmetric stagnation point," PIBAL Rept. 714, ARL Rept. 139, Polytech. Inst. of Brooklyn, Aerodynamics Res. Lab. (September 1961).

Comment on "Planar Librations of an Extensible Dumbbell Satellite"

F. W. NIEDENFUHR*

Ohio State University, Columbus, Ohio

IN his interesting paper,¹ Paul discussed the feasibility of damping the libration mode of an elongated satellite by means of a damper that is coupled to the libration mode through the centrifugal forces due to the libration velocity. Not unexpectedly, it is found that, since the libration mode period is long, the coupling to the damping is not very effective as regards to stopping the libration. The problem is interesting because too heavy a damper will (essentially) couple the elements rigidly and thus have no effect on the libration mode. A different damper configuration that appears to have a more effective coupling between the system modes is suggested in Fig. 1, where a simplified dumbbell is shown consisting of equal masses m connected by a weightless rod of length $2a$. The angle θ shown is the libration angle measured from local vertical. To damp the libration, a symmetrical flywheel of polar moment of inertia I may be attached at the mass center of the satellite. This flywheel may turn freely with respect to the dumbbell, except insofar as it is restrained by the viscous damper indicated in the figure. Denoting the rotation of the flywheel with respect to local vertical by φ , equations of motion of the system easily are found to be

$$\begin{aligned} \ddot{\theta} + (c/2ma^2)\dot{\theta} + 3\Omega^2\theta - (c/2ma^2)\dot{\varphi} &= 0 \\ -(c/I)\dot{\theta} + \ddot{\varphi} + (c/I)\dot{\varphi} &= 0 \end{aligned} \quad (1)$$

where dots indicate time differentiation, and Ω is the orbital circular frequency, just as in Ref. 1. Assuming solutions of the form

$$\theta = \Theta e^{\lambda t} \quad \varphi = \Phi e^{\lambda t} \quad (2)$$

the characteristic equation of the problem is found to be

$$\lambda^4 + (c_1 + c_2)\lambda^3 + 3\Omega^2\lambda^2 + 3\Omega^2c_2\lambda = 0 \quad (3)$$

where $c_1 = c/2ma^2$, and $c_2 = c/I$. Denote the four roots of

Received May 3, 1963.

* Professor of Engineering Mechanics.

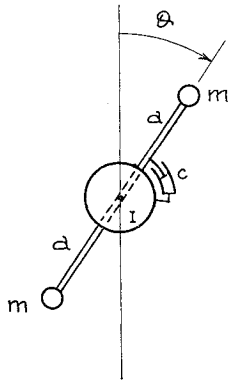


Fig. 1 Idealized dumbbell satellite with damper

this equation by 0, $-\alpha_1$, $-\alpha_2 \pm i\beta$. Forming the quartic that has these roots, one obtains

$$\lambda^4 + (\alpha_1 + 2\alpha_2)\lambda^3 + (\alpha_2^2 + 2\alpha_1\alpha_2 + \beta^2)\lambda^2 + \alpha_1(\alpha_2^2 + \beta^2)\lambda = 0 \quad (4)$$

If now one postulates light damping so that α_2^2 and $\alpha_1\alpha_2$ are small as compared to β^2 , Eq. (4) becomes

$$\lambda^4 + (\alpha_1 + 2\alpha_2)\lambda^3 + \beta^2\lambda^2 + \alpha_1\beta^2\lambda = 0 \quad (5)$$

Identifying the coefficients of Eqs. (3) and (4), one thus finds for the lightly damped case the four roots:

$$\begin{aligned} \lambda_1 &= 0 & \lambda_2 &\doteq -(c/I) \\ \lambda_{3,4} &\doteq -(c/4ma^2) \pm i3^{1/2}\Omega \end{aligned} \quad (6)$$

The libration mode occurring at circular frequency $3^{1/2}\Omega$ thus appears to be quite well damped. The zero root in Eq. (6) arises because the flywheel is indifferent as to its rest position.

Reference

¹ Paul, B., "Planar librations of an extensible dumbbell satellite," *AIAA J.* 1, 411-418 (1963).

Equations for Specifying Orientation of a Planet-Orbiting Body for Yaw, Pitch, and Roll

J. F. BELL*

The Martin Company, Baltimore, Md.

RECENT developments in satellite design require more detailed analyses of the effects of solar heating on the vehicle—particularly with respect to complex motions, where yaw, pitch, and roll are significant.

Katz,¹ in his paper on solar heating, developed equations describing the orientation of an orbiting body referenced to its orbital plane; however, this paper did not contain equations that would describe the orientation of a spinning body in orbit which has been yawed and pitched or subjected to other complex motions. This paper contains equations that will permit consideration of a spinning, yawed, and pitched body.

Received March 27, 1963. The writer wishes to express his thanks and appreciation to Robert H. Swope of the Johns Hopkins Applied Physics Laboratory and to W. Coleman Guthrie of the Martin Company for their many helpful suggestions, comments, and criticisms during the preparation of this manuscript.

* Propulsion Engineer, Propulsion and Thermodynamics Department. Member AIAA.

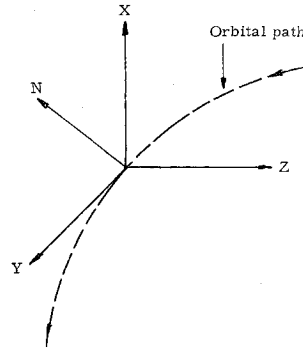


Fig. 1 Orientation of X , Y , and Z axes to orbital plane; X lies in orbital plane, is normal to orbital path, and points outward from orbital path; Y lies in orbital plane, is tangent to orbital path, and points in direction of body travel; Z forms a right-hand vector system with X and Y ; N is a surface normal to any element area at body surface

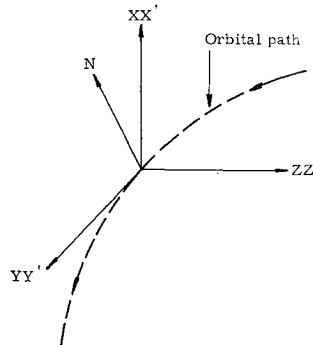


Fig. 2 X' , Y' , and Z' body axes coincident with X , Y , and Z axes at perigee, with no yaw, pitch, or spin

The general case of motion for an orbiting body, of course, would consider not only yaw, pitch, and spin but also periodic (oscillatory) motions, with and without damping. However, periodic damped or undamped motion will not be considered here, except insofar as spin may be thought of as a continuous periodic roll.

For convenience, definitions of yaw and pitch will be taken as fixed angular displacements about particular axes of rotation; spin will be taken as continuous body roll about a particular axis. In general, the definitions, as given below, will follow standard aerodynamic practice. Orientation of the unprimed X, Y, Z axes with respect to the orbital plane is shown in Fig. 1.

For the case in which an orbiting body is not yawed, pitched, spun, or subjected to other motions (Fig. 2), the orientation of any body element surface area normal is specified with respect to the X, Y, Z axes at perigee, by the angles α, β , and γ , respectively. However, when a body is subjected to motions such as yaw, pitch, and spin, the angles α, β , and γ may change by a fixed amount or continuously, such that some means must be devised to describe the orientation of body element surface area normals at any instant of time.

Yaw will be considered as a fixed angular displacement, always taken about the X axis (Fig. 3). Pitch will be considered as a fixed angular displacement about the Z' axis. This axis is referenced to a coordinate system, which is fixed with respect to the orbiting body (Fig. 3). Spin is taken as a continuous body roll about the Y' axis, which is referenced to the rotating body coordinate system (Fig. 3). The same assumptions are made here as are made in Ref. 1, with respect

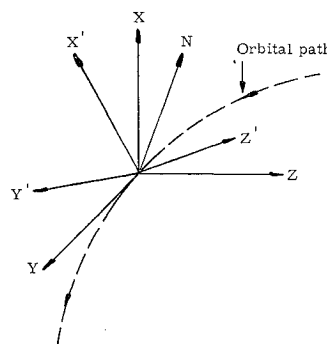


Fig. 3 X' , Y' , and Z' axes noncoincident with X , Y , and Z axes, with yaw, pitch, and spin